Lagrangian Motions and Global Density Distributions of Floating Matter in the Ocean Simulated Using Shipdrift Data

Y. WAKATA* AND Y. SUGIMORI

Faculty of Marine Science and Technology, Tokai University, Shimizu Shizuoka, Japan

(Manuscript received 10 April 1989, in final form 14 August 1989)

ABSTRACT

The Lagrangian motions of floating matter on the sea surface were simulated by using the surface current data based on shipdrift data produced by Meehl. The validity of the simulation was confirmed by comparing the results of the model with the trajectories of satellite tracked drift in the eastern North Pacific observed by Kirwan et al. Some cases which originated in the western North Pacific Ocean were investigated. It was found that drifters set in the ocean during spring quickly migrated to North America on the strong eastward North Pacific currents of the summer season. Trajectories started during autumn showed a loop in the western North Pacific and took more time to arrive in the eastern area of the North Pacific Ocean. Each trajectory that arrived in the eastern area of the North Pacific Ocean, showing a large loop, traveled over a one year interval owing to the large surface current vortex. This vortical sea surface current was driven by the clockwise winds around the atmospheric subtropical high pressure region located in the North Pacific.

Numerous calculations with initial positions randomly scattered in space and time were performed, and the accumulated matter density was obtained. High density areas where the debris concentrated were found at several places (i.e., near Bermuda, west of Australia, the center of the South Atlantic, and north of the Hawaiian Islands). In focussing on the North Pacific, it was found that three identifiable high density areas circulate with three year periods. It is emphasized that the instantaneous strong convergence areas do not always agree with the high accumulation density areas owning to the hysteresis or memory of the floating debris.

1. Introduction

The main goals of this study are to determine where oceanic floating matter gathers and when the concentration of such matter becomes high. Material transport by ocean currents is an important problem in the pollution of the environment as well as in ocean physics. Floating debris, such as fishing nets and gear discarded or lost from fishing vessels, becomes an important factor in environmental pollution. It is also of interest for ocean physics since it acts as a tracer of surface currents. Recently the Fisheries Agency of Japan conducted research of floating debris in the North Pacific and obtained the density distribution of floating matter by sighting observations (Mio and Takehama 1988). It was found that debris concentrated at a location north of the Hawaii Islands.

In this paper, the Lagrangian motion of floating matter was simulated and the density distribution was obtained from a number of simulations. Due to the shortage of surface current data, few people have tried to simulate Lagrangian motion in the ocean. The simulations were produced using the global surface current dataset based on shipdrift observations compiled by Meehl (1982). The validity of the model was confirmed by comparing the model results with drifter observations compiled by Kirwan et al. (1978b). Several North Pacific trajectories, which originate near Japan, are investigated. Differences in trajectories that started in different seasons are discussed.

Further, by assuming that debris discarded from many fishing vessels are homogeneously distributed in the ocean, the accumulation areas, owing to the intrinsic property of oceanic surface currents, can be investigated. The trajectories, a total of 7755, from homogeneously scattered initial points and times were simulated over two years of integration time, corresponding to the estimated lifetime of the debris. The high density locations are defined, and the mechanism of the accumulation of debris is discussed by comparing the simulations with the convergence of surface currents.

2. Shipdrift data

The global surface currents of the ocean are still not sufficiently understood. They may be directly driven by the surface winds and consist of an Ekman component in addition to geostrophic currents. Therefore,

* Present affiliation: Joint Institute for the Study of the Atmosphere and Ocean. University of Washington.

Corresponding author address: Dr. Y. Wakata, Joint Institute for the Study of the Atmosphere and Ocean, AK-40, University of Washington, Seattle, WA 98195.

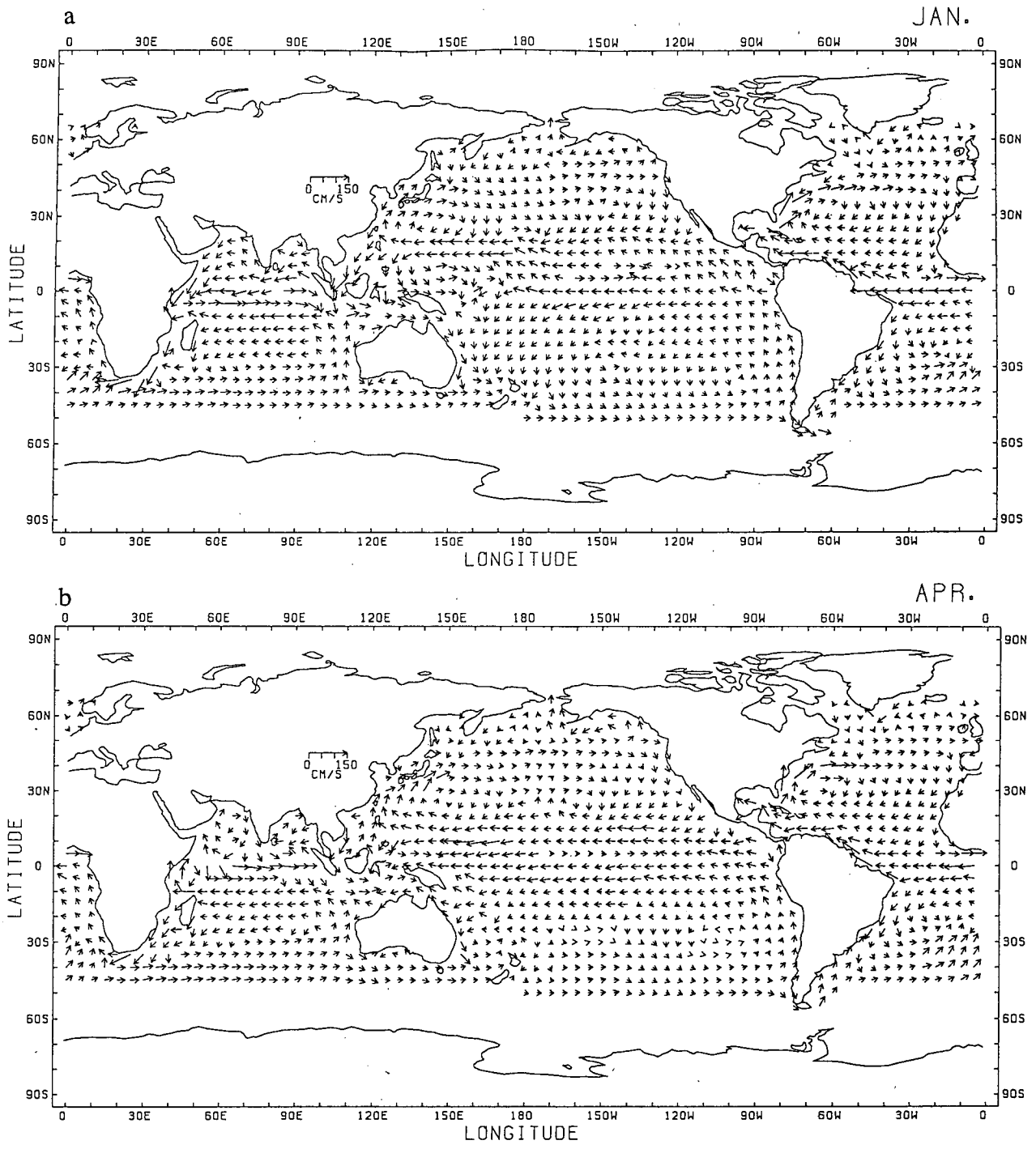

FIG. 1. Sea surface currents obtained from shipdrift data: (a) January, (b) April, (c) July, (d) October.

they differ somewhat from the geostrophic current. In fact, Wyrtki (1975) showed a less direct correspondence between surface winds and the geostrophic currents in the tropical Pacific. Further, Kirwan et al. (1978b) and Harris and Stavopoulos (1978) discussed that drifter speeds representing surface currents were about twice as large as the calculated geostrophic currents.

For the purpose of investigating the movement of floating matter, use of the directly observed data of surface currents rather than the geostrophic current is appropriate. This type of dataset was produced by Meehl (1982). He compiled a digitized dataset of surface currents by reading the shipdrift data from pilot charts of U.S. Naval ships. His results correspond well

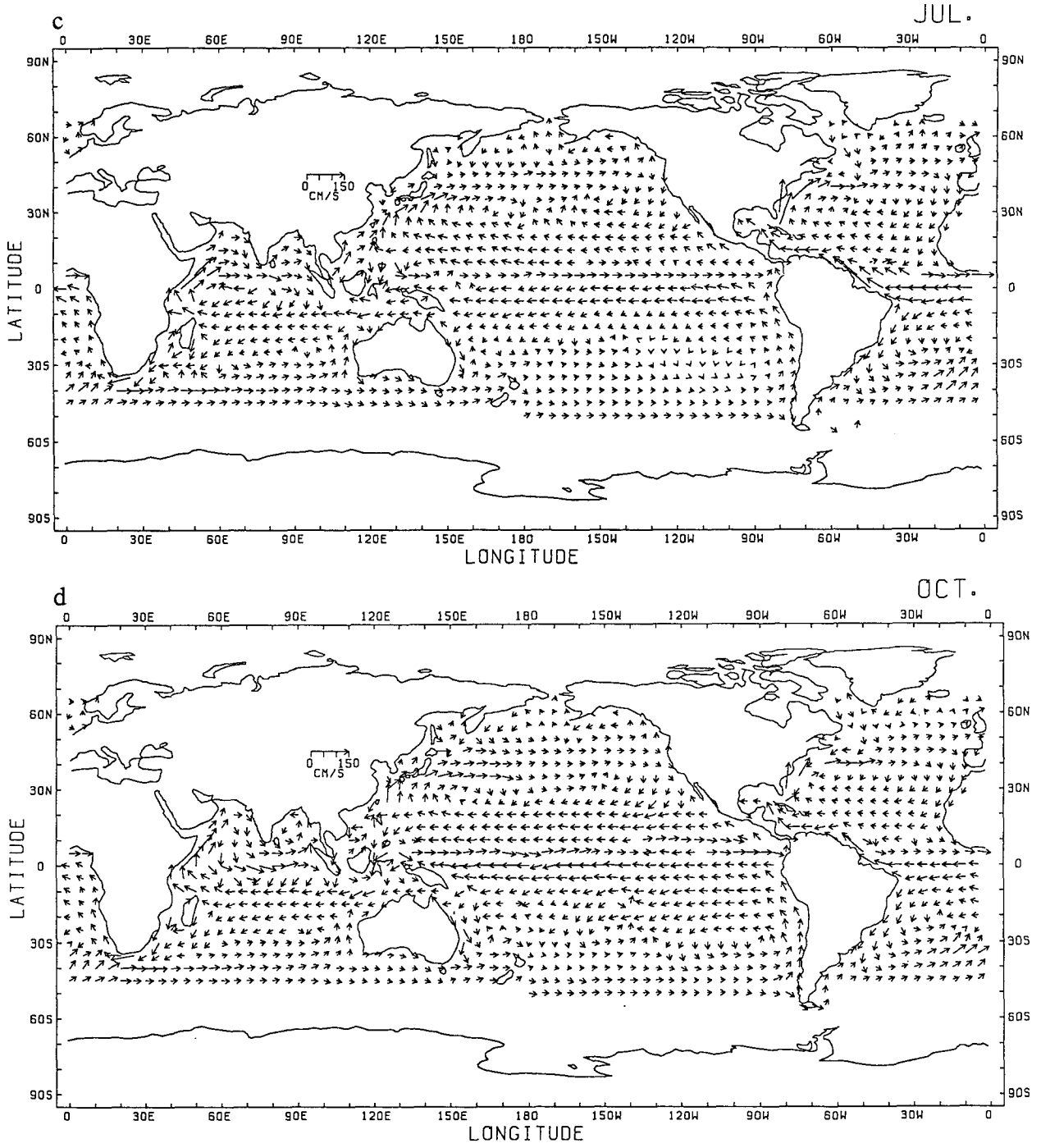

FIG. 1. (*Continued*)

to the drifter movement in magnitude and orientation. It is thought that this shipdrift dataset is more suitable for the present discussion on the Lagrangian motion of floating matter.

The original pilot charts are depicted in 12 monthly charts for the North Atlantic, North Pacific and Indian Ocean and in four seasonal maps for the South Atlantic and South Pacific. Meehl (1982) then composed the global dataset of surface currents for the four midseason months represented by vectors on a 5° by 5° latitude–longitude grid. The maps of surface currents are depicted in Fig. 1 for the four midseason months.

Two closed gyres in the North Pacific Ocean are seen in Fig. 1, which are also seen in the maps of

streamlines depicted in Meehl (1982), and discussed by Sverdrup et al. (1942). These gyres play an important role in the accumulation of debris as will be discussed later. The western gyre is also seen in maps of dynamic topography depicted by Reid (1961) and Wyrtki (1975), but the eastern gyre is not found in their maps. Taking into account the difference between geostrophic current and surface flow, this discrepancy is understandable.

This eastern gyre results from the North Pacific subtropical high pressure area. The gyre center shifts northward during the summer season as shown in Fig. 1c. In fact, it is found that the center of the eastern gyre coincides with the center of the wind vectors around the North Pacific subtropical high pressure area shown in Fig. 2. This wind map was produced by averaging the NMC July monthly mean wind data from 1968 to 1985. Further comparison of the wind and current vectors shows that the current direction is generally to the right of the downwind direction in the Northern Hemisphere and to the left in the Southern Hemisphere. This agrees with the observation compiled by McNally (1981) and McNally and White (1985). They found that drifters moved at approximately 30 degrees to the right of the surface wind vector. The theoretical Ekman component of the surface current due to wind stress is 45° to the right (left) of the downwind direction in the Northern (Southern) Hemisphere.

The western gyre increases in strength during the winter season, developing strong southward currents. This plays an important role on the trajectory of a drifter.

3. The model

The trajectory of a floating drifter is calculated by solving the Lagrangian equation in spherical coordinates

$$\frac{d\theta}{dt} = \frac{1}{a\cos\lambda} U(\lambda, \theta, t),$$

$$\frac{d\lambda}{dt} = \frac{1}{a} V(\lambda, \theta, t),$$

where λ, θ and t are latitude, longitude and time, respectively, and a is the earth's radius. If the velocities U and V are known at any point in space and time, the movement of the drifter can be predicted by solving the above equations.

The velocity at a given time at a grid point can be obtained by using the third-order spline interpolation method. The data for each month in Meehl (1982) were taken at the 15th of each month, i.e., the data of January were set at 15 January. The interpolation in time was done by using the spline method, resulting in nine midseason months of data (i.e., almost two years) before and after the month of a time calculation, in order to avoid the error due to the edge of an interpolation area. The velocity at a position not falling on a grid point was interpolated linearly from the surrounding four data points, which were already inter-

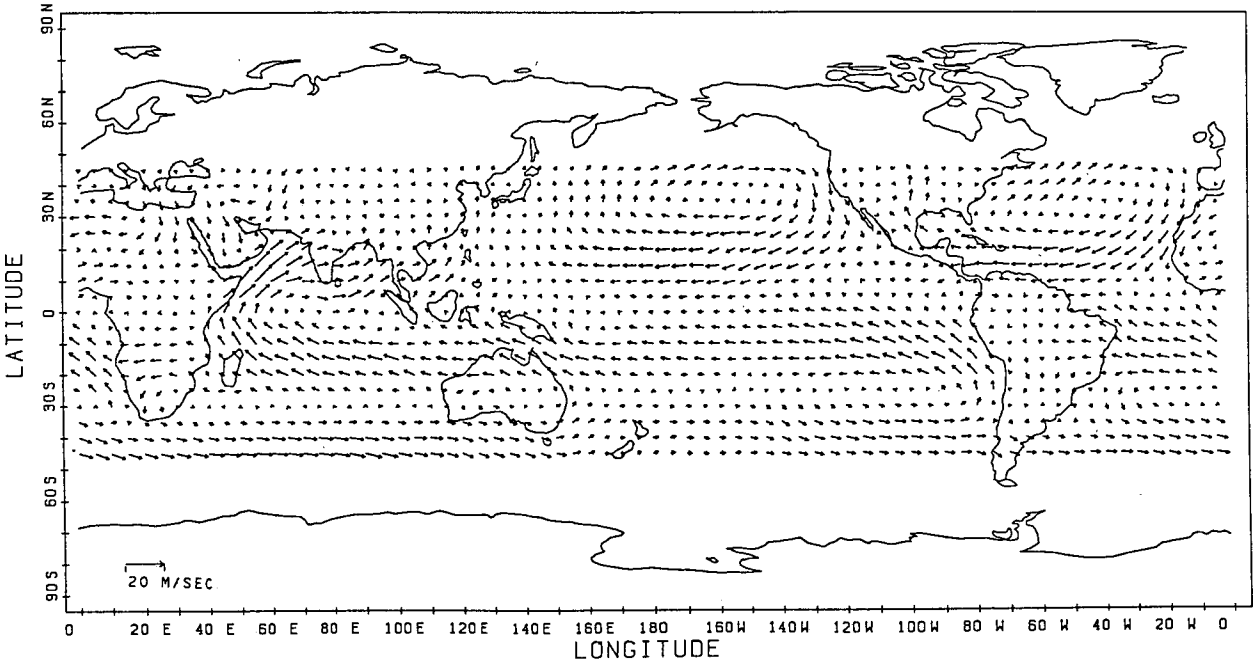

FIG. 2. Wind vectors in July at the 1000 mb level produced by averaging the July NMC datasets from 1968 to 1985.

polated in time to the grid points. The current velocities for any time and space on the earth's ocean surface can be obtained by use of these interpolation procedures. The above Lagrangian equation was calculated using the Runge Kutta scheme with a time difference of 3 days.

It should be emphasized that Meehl's data are the long-term mean ocean current flow, and at any particular instant the current velocity would undoubtedly differ from the mean. Instantaneous flow would probably show a series of eddies superimposed on the general mean flow. Therefore, the present results should be interpreted as the ensemble mean of many drifter trajectories.

4. Simulation of Lagrangian motion

Kirwan et al. (1978b) observed the trajectories of 22 drifters in the eastern North Pacific tracked by the Nimbus-6 satellite during the period 10 September 1976 through 31 August 1977. Their trajectories defined the eastern portions of the subarctic and subtropical gyres and showed the split between these gyres which occurs between 45° and 50°N at 140°W.

The simulations are performed in order to compare the model results with the observations. Three initial drifter release points are chosen along 165°W longitude at 50°, 45° and 40°N latitude. The integration period was taken between 10 September and 31 August in the year corresponding to the period of the observation. The results depicted in Fig. 3 show the presence of two gyres. The trajectory that originated at 45°N passes between the subtropical and subarctic gyres, and reaches the west coast of North America, stopping at this stagnation point. The speed of the simulated drifter is somewhat faster than that observed, but the overall results agree very well with the observed trajectory shown in Fig. 3 of Kirwan et al. (1978b). Thus, the model is thought to be reliable for the simulation of the floating matter.

The circulation of floating matter in the North Pacific was investigated. The initial point was selected as a point 30°N, 150°W near Japan. The differences in trajectory with respect to the season in which the drifter was first set in motion as shown in Fig. 4a–d are discussed.

- The calculation shown in Fig. 4b started on 1 April (spring), i.e. the drifter was released on this date. Upon release, it migrated eastward and reached the date line within half a year. After reaching the date line it moved in a loop near 30°N, 150°W in the eastern North Pacific, and remained there for about two years.
- The simulated trajectory of a drifter released on 1 June (summer) is shown in Fig. 4c. The speed of the eastward migration is faster than the spring case, reaching the date line in only about four months. In autumn the eastward current near 140°E is the fastest. The drifter that starts in the summer would follow this fast current in autumn. After that it wanders north of Hawaii Islands.
- Figure 4d shows the simulated result of a drifter released on 1 October in autumn. The drifter curved southward owing to the strong southward current and westward return flow during the winter shown in Fig. 1a and makes a large loop in the western part of the North Pacific.

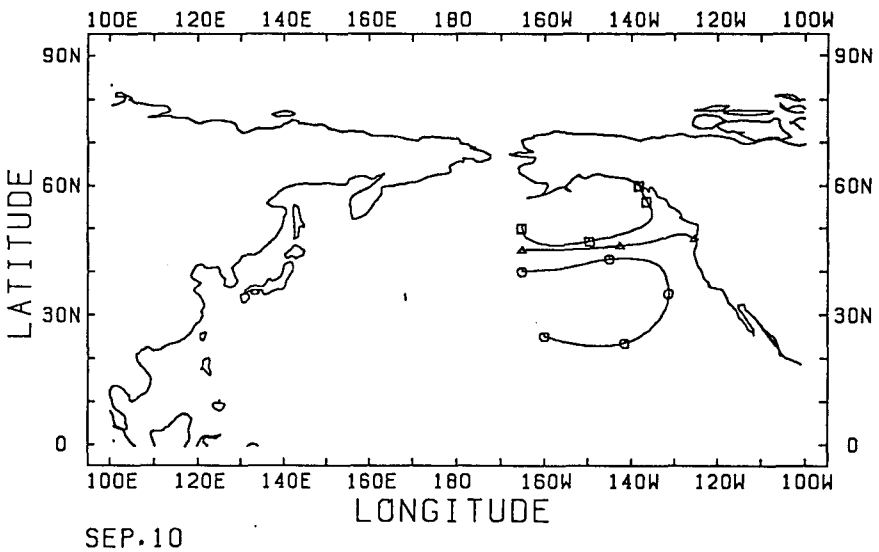

FIG. 3. Simulated trajectories of drifters originating at three points (40°N, 165°W), (45°N, 165°W) and (50°N, 165°W). The calculation was performed for 10 September to 31 August. Interval between marked points is three months.

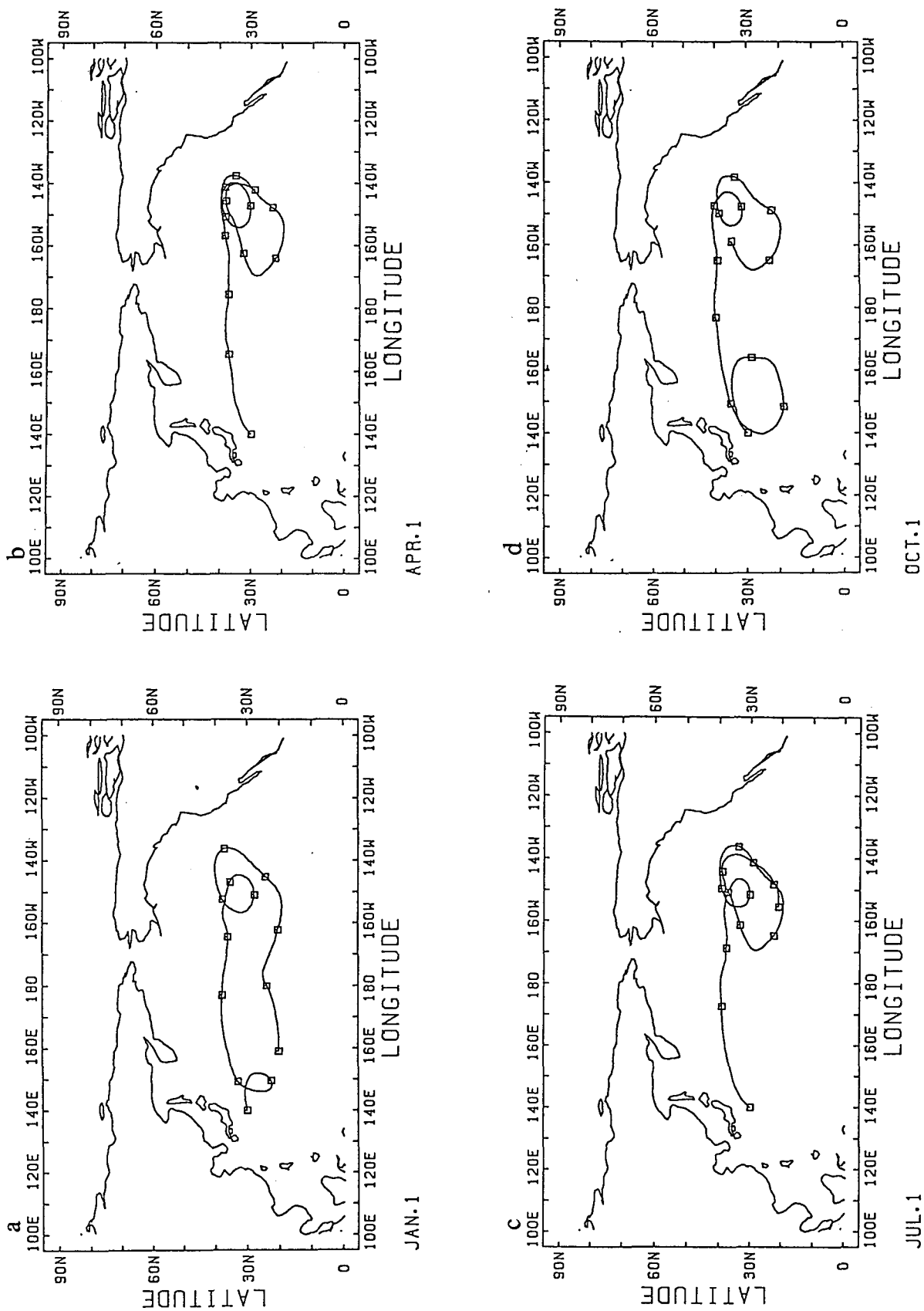

FIG. 4. Trajectories originating from an initial point near Japan (30°N, 40°E) during (a) 1 January, (b) 1 April, (c) 1 July, and (d) 1 October. The interval between the marked points is three months.

• In the case shown in Fig. 4a, when the drifter released on 1 January (winter), the western loop becomes small.

All of these cases showed the large loop in the eastern North Pacific. This means that the drifter stays in the loop a long time, indicating that the density of floating debris may become high, as shown in observations by Mio and Takehama (1988).

5. Density distribution of floating matter

Several trajectories of floating matter were simulated in the previous section. However, determination of the accumulation of floating matter cannot be made on the basis of only a few simulated trajectories. In this section, the areas where debris gathers are obtained directly from simulating many trajectories. To seek the places where debris are likely to accumulate, the initial releases for the calculations are scattered homogeneously in space and time. In this way, the accumulation must be due to ocean currents and not to the input conditions.

In all, 7755 trajectories were calculated. The starting positions are randomly set for a uniform number per unit area over both land and ocean. If random numbers are generated using longitude and latitude (θ, λ) as variables, the density becomes large in high latitude regions. Therefore, a new variable $\xi = \sin\theta$ is introduced, yielding an equal area element. The generation of the random positions is now homogeneous in the variables (ξ, λ) in space from 70°S to 70°N. The initial positions in longitude and latitude can be obtained by the inverse transformation from these new variables.

By this procedure, the density of the initial points becomes uniform, $5/(3.09 \times 10^{11}\ \mathrm{m}^2)$, which corresponds to five drifters per square of 5° × 5° at the equator. The initial times are also scattered over four years, so that any preferred season for the accumulation of debris does not depend on the distribution of initial seasons. The floating debris is assumed to have a lifetime, since the elements of the debris may become rotted or become attached to seaweed and shellfish and sink into the deep ocean. This lifetime is assumed to be two years. The calculations are performed over a two year interval from random starting times scattered over four years. The drifters begin to disappear after two years. The total amount of floating matter at a given instant increases monotonically from the start of the calculation until the second year, since no simulated drifters have disappeared in this interval. From the third year to the fourth year the total number becomes constant at about 3875, since the input and disappearance rates approximately balance. Finally, from the fifth to the sixth year the density decreases monotonically, since there is no longer any input.

We will discuss the equilibrium material density over the interval from the third to the fourth year. The material density each season of the third year agrees very well with that of the fourth year. This result guarantees the homogeneity of the initial points, and that the total number of drifters chosen is sufficient. Figure 5 shows the material densities for each season of the third year. The points are scattered homogeneously on land, while the highly dense regions can be seen in the oceans owing to the sea surface currents. There are notable accumulation areas around Bermuda, the center of the South Pacific Ocean, and the region west of Australia. In the North Pacific, an area we will concentrate on, accumulation areas are found in the eastern basin, with the areas shifting a bit during each season. Another accumulation area is found west of Borneo where the north equatorial current becomes weak.

The convergence of surface currents for each season is shown in Fig. 6. The intense convergence region in the eastern North Pacific Ocean is found at 35°N, 160°W in summer. This region agrees with the center of North Pacific atmospheric subtropical high shown in Fig. 2. This can be easily understood since the wind around high pressure areas in the Northern Hemisphere rotates clockwise and the Ekman currents of ocean are directed to the right of the downwind direction.

Comparing the convergence fields shown in Fig. 6 with the density fields, we see that the intense convergence regions do not always agree with the high density regions. Good agreement between these two fields is seen in some regions, such as at the center of the South Atlantic Ocean where the convergence fields do not vary much in time. However, the convergence fields generally do vary in time, and matter that once accumulates subsequently migrates by advection. If the lifetime of the floating debris is short, these two fields may agree. However, floating matter having a long life time has been affected by past flows and therefore has a hysteresis. It should thus be emphasized that simply inferring the density from the convergence fields of the flow may be misleading.

The density distributions in the North Pacific Ocean for each month is shown in Fig. 7. Comparing the density field of each month, it is found that some highly dense regions migrate as a group and can be traced. One high density region marked A in January at 20°N, 160°E in the western North Pacific Ocean migrates westward on the north equatorial current, is carried northward by the Kuroshio Current, and then slowly migrates eastward on the North Pacific current, all occurring over a one year interval. The behavior of the next year can be obtained from these successive figures, since the density distribution in the equilibrium state is cyclic in behavior with a one year period owing to the annual periodicity of the currents. The high density area of the following year is marked by a B. This B area becomes stagnant around the eastern North Pacific after about one year. In the following year the high density region marked by C again migrates westward on the north equatorial current for about one year and

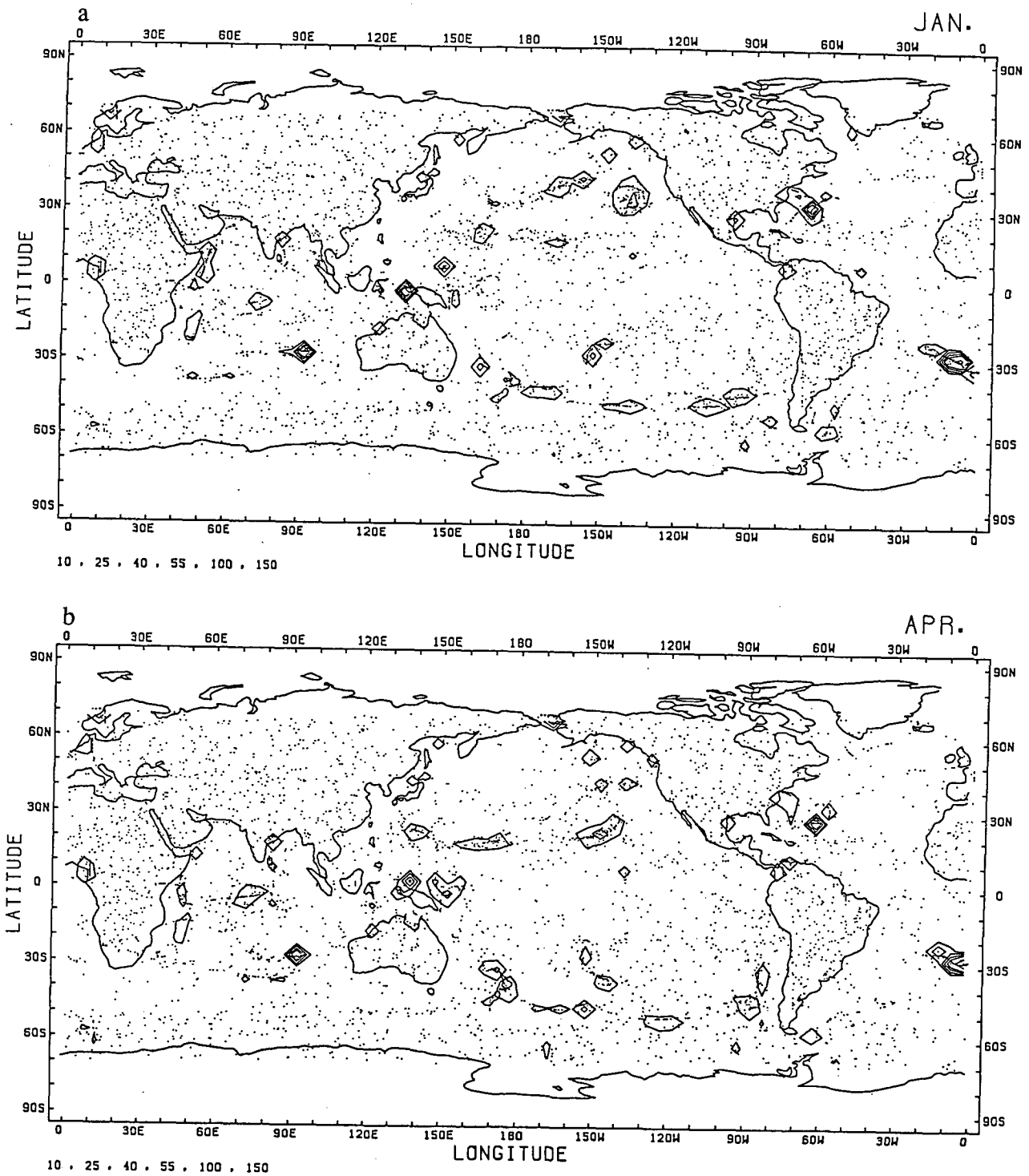

FIG. 5. Global density distribution for each season: (a) 15 January, (b) 15 April, (c) 15 July, (d) 15 October. The contour values are 10, 25, 40, 55, 100, and 150 which is the number of matter per 5° × 5° square at the equator.

is succeeded by area A. It was found from the above results that three identifiable high density regions are always present and circulate with a three year period in the North Pacific Ocean. One of these always stagnates in the eastern North Pacific Ocean and composes the high density region north of the Hawaii Islands observed by Mio and Takehama (1988).

This result can be analogously understood by imagining three trains with passengers running in the North Pacific Ocean. The intense convergence regions in the

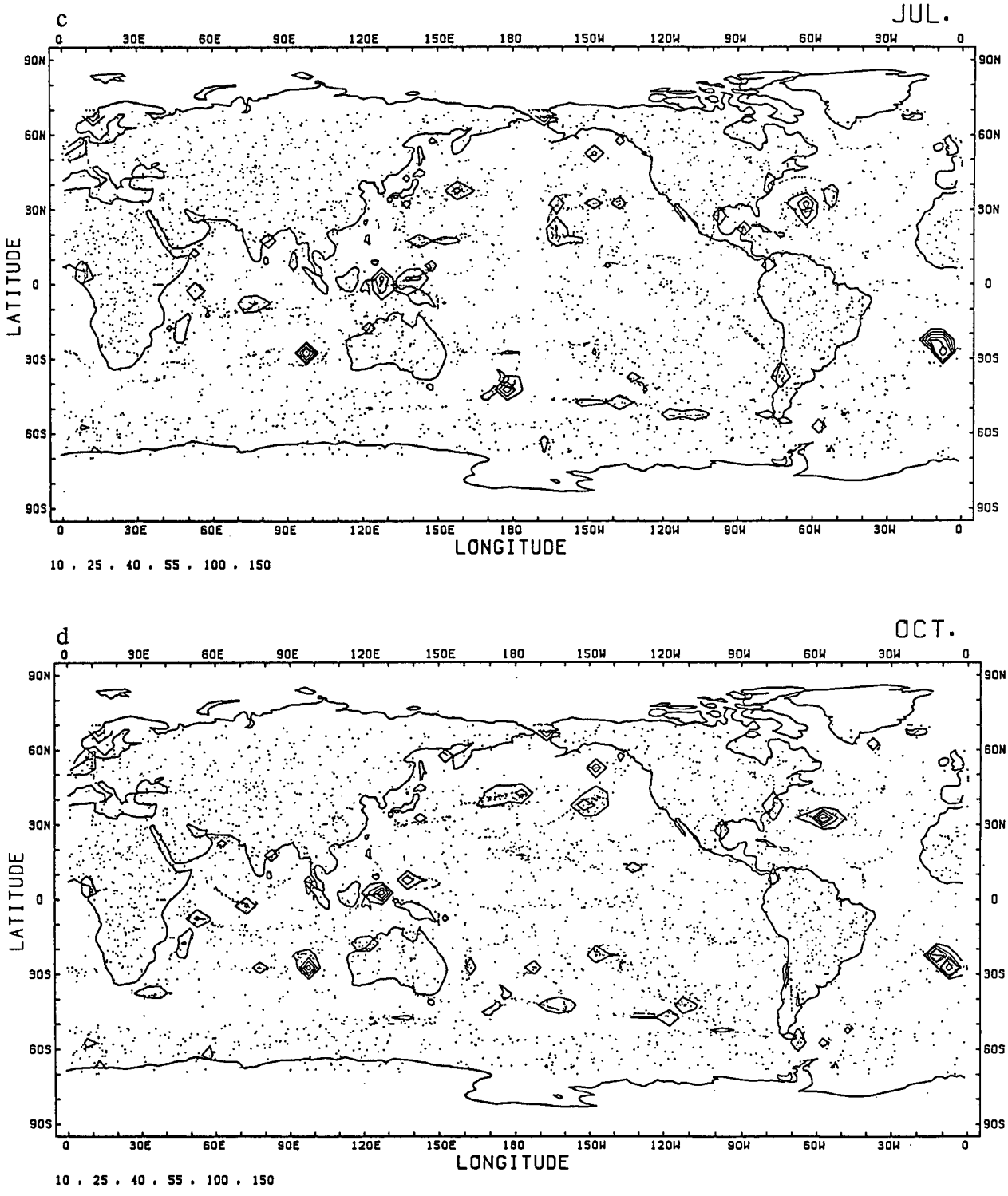

FIG. 5. (*Continued*)

eastern part of the North Pacific around 30°N, 160°W due to the summertime North Pacific subtropical high pressure area and the region east of Japan in summer are entraining stations, while the other regions are detraining stations. The number of passengers boarding a train depends on the stopping time at each station. The train takes on the passengers in the region east of Japan and travels eastward. Arriving in the eastern

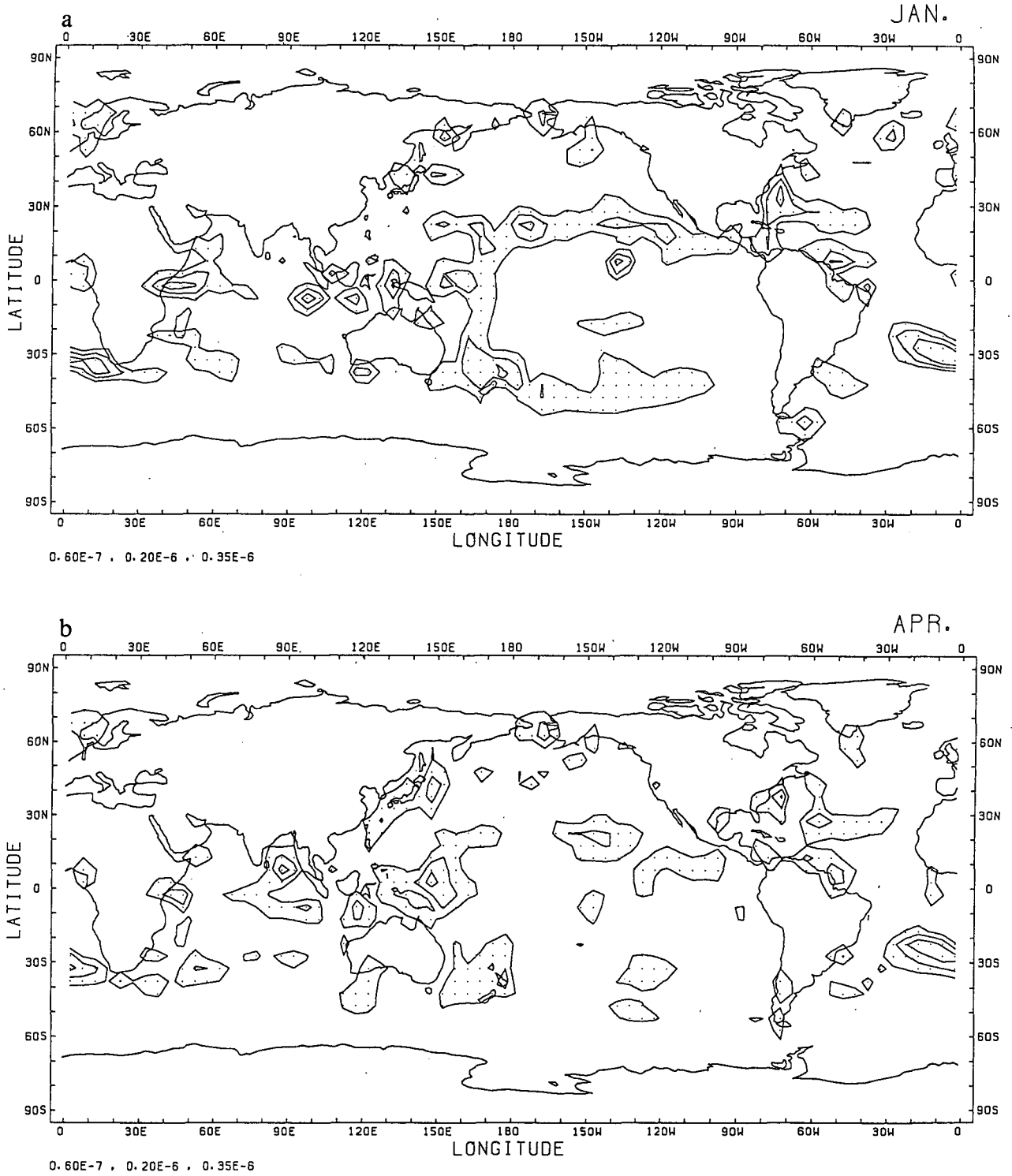

FIG. 6. Convergence fields for each season. (a) January, (b) April, (c) July, (d) October. The contour lines are 0.60×10^{-7} s^{-1}, 0.20×10^{-6} s^{-1} and 0.35×10^{6} s^{-1}.

North Pacific Ocean, the train remains about one year and takes on many passengers, the last in summer. The full train moves southward and then migrates westward letting the passengers off over a period of one year. Therefore, three trains circulate around the North Pacific Ocean over a three year period. The passengers do not go around the North Pacific Ocean but the train does, since the lifetime of matter is only two years. It

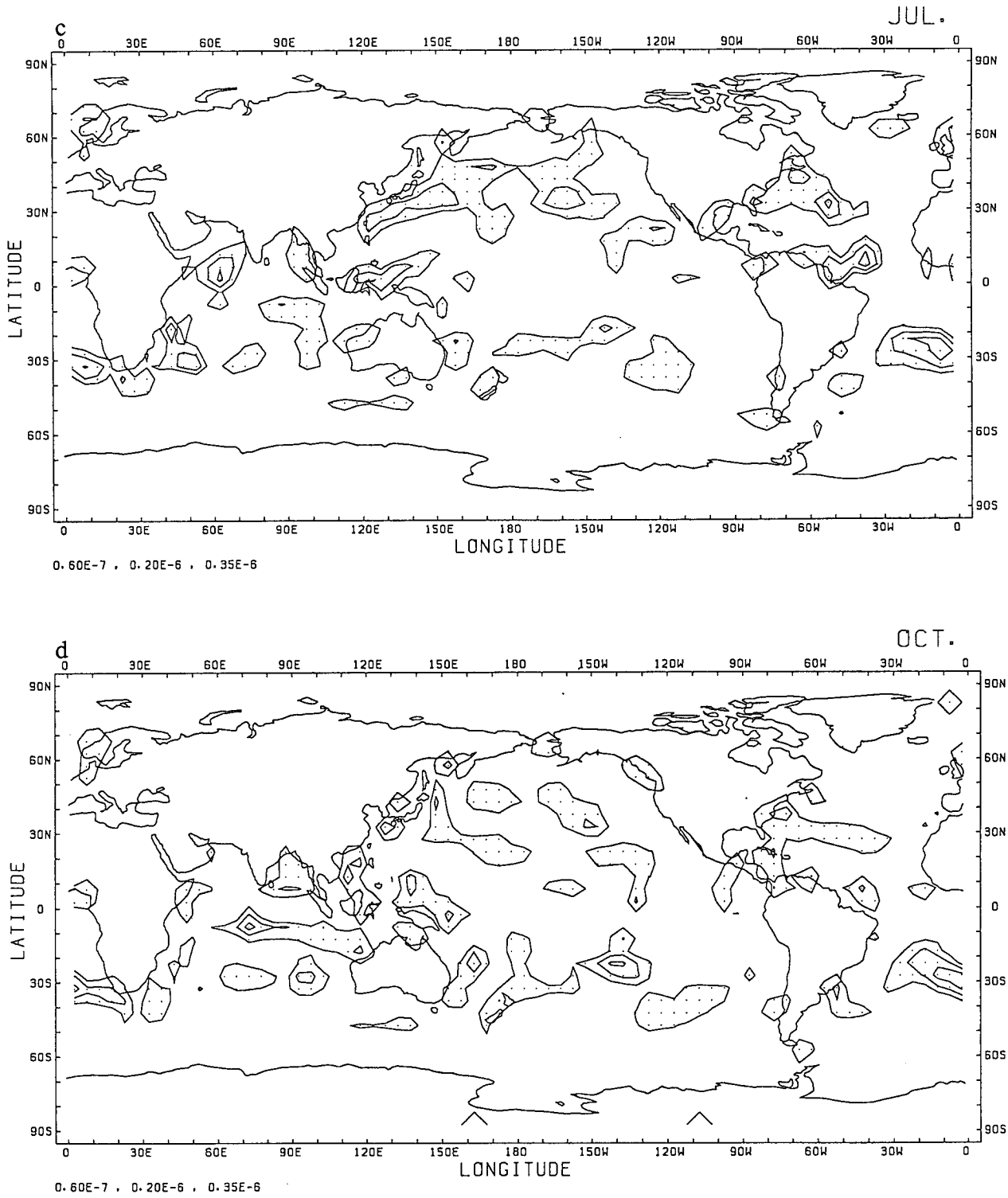

FIG. 6. (*Continued*)

should be emphasized that the train can be traceable in spite of the exchanging of the passengers. From this fact it can be inferred that the present scenario does not, to a great extent, depend on the lifetime of debris. If the lifetime of the debris is long or short, the train becomes more or less crowded, accordingly.

The circulation period of high density area may depend on the properties of the surface current data.

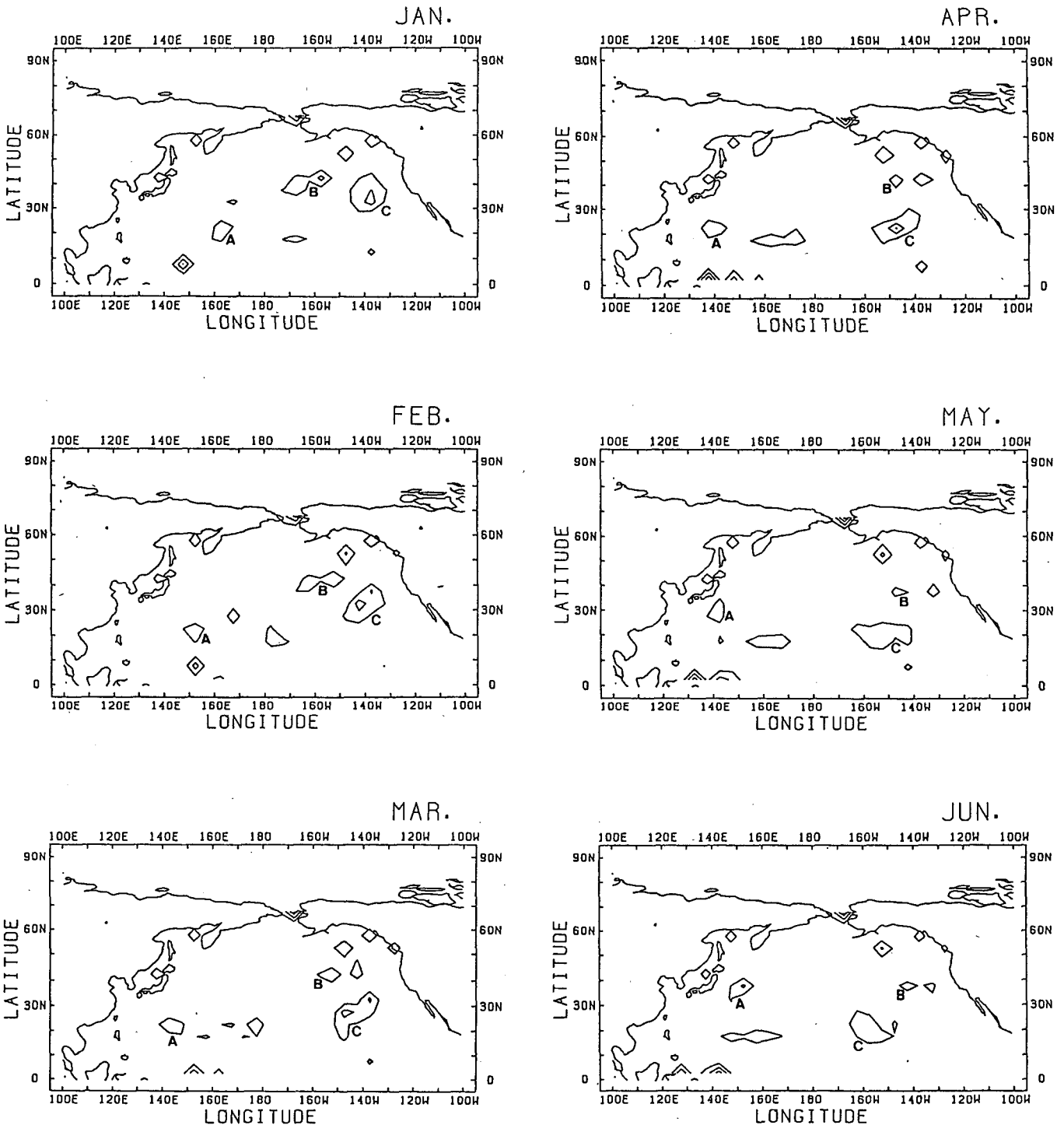

FIG. 7. The monthly density distribution in the North Pacific Ocean. Contour lines are as in Fig. 5.

However, it should be emphasized that for the appearance of traceable groups of high density areas circulating in the North Pacific Ocean, the strength of the surface convergence must vary in time. The period of the circulation of these groups must be a multiple of one year, owing to the annual variation of currents. Furthermore, in order that the densities of the debris have an annual variation, the number of circulating groups must be numerically equal to the period (in years) of the group circulation. If the lifetime of the debris is shorter than this period of the group circulation, the high density groups would disappear were

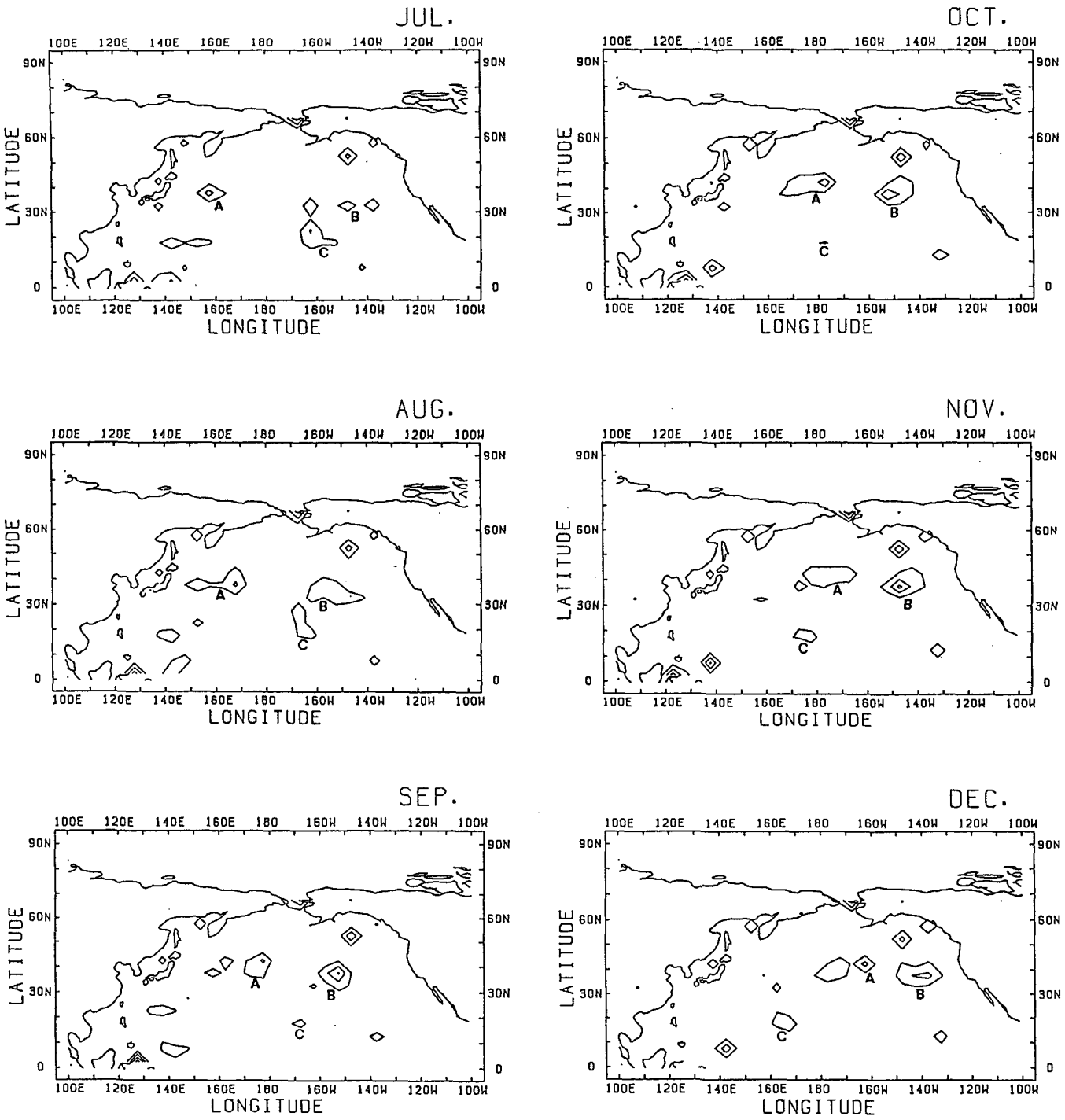

FIG. 7. (*Continued*)

it not for the convergence, which concentrates different drifters into the circulating regions.

6. Summary and discussion

The trajectory and density distributions of floating debris were investigated using shipdrift data. The simulated drifters originating from points near Japan during the summer season undergo a fast migration to the eastern North Pacific Ocean, while the drifters originating in the winter season complete a large loop in the western North Pacific Ocean and therefore take a long time to arrive in the eastern Pacific.

Numerous trajectories were calculated from initial points scattered homogeneously in time and space to

seek the density distribution of floating matter. It was found that debris accumulates around Bermuda, at the center of the South Atlantic Ocean, to the west of Borneo, and to the west of Australia. Further, three traceable high density regions are found in the North Pacific Ocean, the group migrating around the Pacific with a three year period. One is always present north of Hawaii, which corresponds to the sighting observation by Mio and Takehama (1988). It was found that the floating debris accumulated by the intense convergent flow driven by the winds associated with the atmospheric North Pacific subtropical high.

It should be noted that an intense convergence area is not always a high density debris area. For example, the season of intense convergence is not simply the high density season, since matter is continually accumulating. Thus, the density becomes maximum when the convergence becomes zero. Further, the movement of matter is affected by the advective properties of the current. Thus the high density regions migrate as a group, and it may be possible that the density becomes high in the current's divergent areas. Therefore, the simple connection of accumulation and convergence is absent and the time-dependent calculation of density is necessary.

In a future paper, the behavior of material density will be investigated by solving the advection–diffusion equation. The results in this paper were obtained by the use of shipdrift data. In future work, they will be examined by using more detailed observational dataset, along with global circulation models.

Acknowledgments. The authors would like to express their sincere thanks to Dr. M. Kubota of Tokai University, Messrs. S. Takehama, S. Matumura and Dr. S. Mio of the Fisheries Agency of Japan, Dr. G. A. Meehl of NCAR and Dr. E. S. Sarachik of University of Washington for their encouragement and valuable comments. Also, they appreciate the work of the first author's students, Messrs. K. Sugiyama, K. Honda and Y. Masuda, for assisting in the numerical calculations. This research was supported in part by the Fisheries Agency of Japan and a grant from the NOAA Office for Climate of Atmosphere Research to the University of Washington Experimental Climate Forecast Center. The numerical computations were performed with the use of the FACOM M3500 at Tokai University.

REFERENCES

Harris, T. F. W., and C. C. Stavopoulos, 1978: Satellite-tracked drifters between Africa and Antarctica. *Bull. Amer. Meteor. Soc.*, **59,** 51–59.

Kirwan, A. D. Jr., G. McNally and S. Pazan, 1978a: Wind drag and relative separations of undrogued drifters. *J. Phys. Oceanogr.*, **8,** 1146–1150.

——, ——, E. Reyna and W. J. Merrell, Jr., 1987b: The near-surface circulation of the eastern North Pacific. *J. Phys. Oceanogr.*, **8,** 937–945.

McNally, G. J., 1981: Satellite-tracked drift buoy observations of the near-surface flow in the eastern mid-latitude North Pacific. *J. Geophys. Res.*, **86,** 8022–8030.

——, and W. B. White, 1985: Wind driven flow in the mixed layer observed by drifting buoys during autumn-winter in the mid-latitude North Pacific. *J. Phys. Oceanogr.*, **15,** 684–694.

Meehl, G. A., 1982: Characteristics of surface current flow inferred from a global ocean current data set. *J. Phys. Oceanogr.*, **12,** 538–555.

Mio, S., and S. Takehama, 1988: Distribution and density of marine debris in the North Pacific based on sighting survey in 1987. *Proc. of the 35rd INPEC at Fisheries Agency of Japan.*

Reid, J. L., 1961: On the geostrophic flow at the surface of the Pacific Ocean with respect to the 1,000-decibar surface. *Tellus,* **13,** 489–496.

Sverdrup, H. V., M. W. Johnson and R. H. Fleming, 1942: *The Oceans. Their Physics, Chemistry and General Biology.* Prentice Hall, 1087 pp.

Wyrtki, K., 1975: Fluctuations of the dynamic topography in the Pacific Ocean. *J. Phys. Oceanogr.*, **5,** 450–459.